β-D-N⁴-Hydroxycytidine Is a Potent Anti-alphavirus Compound That Induces a High Level of Mutations in the Viral Genome

Nadya Urakova,[a] Valeriya Kuznetsova,[a] David K. Crossman,[b] Arpine Sokratian,[a] David B. Guthrie,[c] Alexander A. Kolykhalov,[c] Mark A. Lockwood,[c] Michael G. Natchus,[c] Michael R. Crowley,[b] George R. Painter,[c,d] (ID) Elena I. Frolova,[a] (ID) Ilya Frolov[a]

[a]Department of Microbiology, University of Alabama at Birmingham, Birmingham, Alabama, USA
[b]Heflin Center for Genomic Science, University of Alabama at Birmingham, Birmingham, Alabama, USA
[c]Emory Institute for Drug Development, Emory University, Atlanta, Georgia, USA
[d]Department of Pharmacology, Emory University School of Medicine, Atlanta, Georgia, USA

ABSTRACT   Venezuelan equine encephalitis virus (VEEV) is a representative member of the New World alphaviruses. It is transmitted by mosquito vectors and causes highly debilitating disease in humans, equids, and other vertebrate hosts. Despite a continuous public health threat, very few compounds with anti-VEEV activity in cell culture and in mouse models have been identified to date, and rapid development of virus resistance to some of them has been recorded. In this study, we investigated the possibility of using a modified nucleoside analog, β-D-N⁴-hydroxycytidine (NHC), as an anti-VEEV agent and defined the mechanism of its anti-VEEV activity. The results demonstrate that NHC is a very potent antiviral agent. It affects both the release of genome RNA-containing VEE virions and their infectivity. Both of these antiviral activities are determined by the NHC-induced accumulation of mutations in virus-specific RNAs. The antiviral effect is most prominent when NHC is applied early in the infectious process, during the amplification of negative- and positive-strand RNAs in infected cells. Most importantly, only a low-level resistance of VEEV to NHC can be developed, and it requires acquisition and cooperative function of more than one mutation in nsP4. These adaptive mutations are closely located in the same segment of nsP4. Our data suggest that NHC is more potent than ribavirin as an anti-VEEV agent and likely can be used to treat other alphavirus infections.

IMPORTANCE Venezuelan equine encephalitis virus (VEEV) can cause widespread epidemics among humans and domestic animals. VEEV infections result in severe meningoencephalitis and long-term sequelae. No approved therapeutics exist for treatment of VEEV infections. Our study demonstrates that β-D-N⁴-hydroxycytidine (NHC) is a very potent anti-VEEV compound, with the 50% effective concentration being below 1 μM. The mechanism of NHC antiviral activity is based on induction of high mutation rates in the viral genome. Accordingly, NHC treatment affects both the rates of particle release and the particle infectivity. Most importantly, in contrast to most of the anti-alphavirus drugs that are under development, resistance of VEEV to NHC develops very inefficiently. Even low levels of resistance require acquisition of multiple mutations in the gene of the VEEV-specific RNA-dependent RNA polymerase nsP4.

KEYWORDS alphaviruses, antivirals, N-hydroxycytidine, RNA-dependent RNA polymerase, Venezuelan equine encephalitis virus, drug-resistant mutant, lethal mutagenesis

Alphaviruses represent a group of mosquito-borne viruses that are widely distributed on all continents. Most of them are maintained in nature by continuous transmission between mosquito vectors and vertebrates that serve as amplifying hosts.

Based on their geographical distribution, the currently known members of the *Alphavirus* genus are divided into the New World (NW) and the Old World (OW) alphaviruses (1). Although the OW alphaviruses cause less severe diseases characterized by rash, fever, and arthritis, most of the NW alphaviruses exhibit an encephalitogenic phenotype (1). The NW representative members include Venezuelan (VEEV), eastern (EEEV), and western (WEEV) equine encephalitis viruses (2–6). In humans, these viruses cause debilitating diseases, and the overall mortality rates are ~1% (7), 30 to 80% (8), and 1 to 5% (9) for VEEV, EEEV and WEEV, respectively.

Alphaviruses replicate to very high titers in many commonly used cell lines of vertebrate and mosquito origins. They can be produced on a large scale, stored in lyophilized form for a long period of time, and efficiently distributed by aerosol. Moreover, mortality rates are amplified with aerosol infection (10). Therefore, EEEV and some VEEV strains can potentially be used by bioterrorists, and thus they are on the U.S. Select Agents and Toxins list. Nevertheless, despite continuous circulation in Central, South, and North America and the public health threat, no safe and efficient vaccines or therapeutics exist against VEEV or other NW alphavirus infections.

VEEV is a relatively small enveloped virus. Its genome consists of a single-stranded RNA (G RNA) of positive polarity. Upon release into the cytoplasm from the nucleocapsids, G RNA serves directly as a template for the translation of nonstructural proteins that mediate replication of viral G RNA and transcription of the subgenomic RNA (SG RNA). The latter RNA is translated into viral structural proteins that ultimately form infectious, G RNA-containing virions. The nonstructural proteins are initially synthesized as precursor polyproteins P123 and P1234 and are later processed by nsP2-associated protease activity into individual nsP1, nsP2, nsP3, and nsP4. This stepwise processing of the polyproteins regulates synthesis of the negative-strand RNA genome intermediates, G RNAs and SG RNAs (11–13).

To date, many functions of individual nsPs in RNA and virus replication have been identified. nsP2, which exhibits protease and helicase activities, and nsP4, which contains the predicted RNA-dependent RNA polymerase (RdRp) domain (1), attracted most of the attention as possible targets for the development of antiviral drugs. However, few screens have yielded positive results thus far. In one study, the identified CID15997213 compound demonstrated a strong inhibitory effect on VEEV replication *in vitro* and in a small animal model via its targeting of the nsP2 protein and ultimately viral RNA replication (14). Some other quinazolinone-derived molecules also exhibited antiviral activity against VEEV (15, 16). For example, compound ML336 inhibited several VEEV strains in the nanomolar range *in vitro* and also protected mice from a lethal VEEV infection. Although the exact mechanism of action for this compound has not been fully elucidated, the mutations that determined drug-resistant phenotypes of VEEV occurred in nsP2 and nsP4 proteins (15).

Compounds that indirectly interfere with VEEV replication by modifying intracellular processes in the host were also investigated as potential therapeutic options to modulate the course of alphavirus infections (17–20). These included (i) an inhibitor of glycogen synthase kinase-3β (GSK-3β) that governs proinflammatory responses in the host cell (17); (ii) acriflavine, an inhibitor of Ago2 (18); (iii) D-(−) enantiomer of carbodine, which inhibited cellular CTP synthetase and was capable of decreasing the levels of intracellular CTP (19); (iv) VX-497, a reversible uncompetitive inhibitor of inosine-5′-monophosphate dehydrogenase, that demonstrated a moderately negative effect on VEEV replication *in vitro* (20); and (v) selective inhibitors of nuclear export, which enhanced accumulation of the capsid protein in cell nuclei and thus decreased the titers of released VEEV (21). Ribavirin, a broad-spectrum antiviral drug, exhibited a very limited effect against VEEV even if applied at concentrations higher than 500 μM (20).

Although several compounds show anti-VEEV activity in cell culture and in mouse models, it is unlikely that a single drug can be sufficiently potent and/or applied without rapid selection of resistant mutants. Therefore, in this study, we investigated the possibility of using a modified nucleoside analog, β-D-N^4-hydroxycytidine (NHC) as
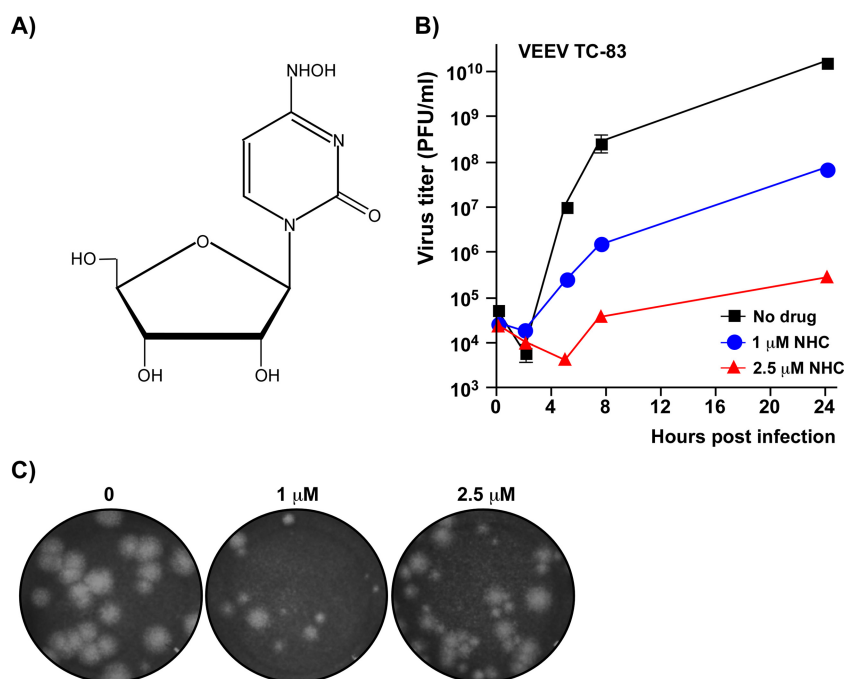
FIG 1 NHC has a strong negative effect on VEEV TC-83 replication. (A) Chemical structure of NHC. (B) Vero cells were infected with VEEV TC-83 at an MOI of 0.5 PFU/cell and were either treated with NHC at the indicated concentrations starting from 0 h postinfection (p.i.) throughout the 24 h of incubation period or they remained mock treated. At the indicated times p.i., media were harvested, and viral titers were determined by a plaque assay on Vero cells. Starting from 5 h p.i., virus titers in the samples harvested from the drug-treated cells were significantly different from those collected from the mock-treated cells ($P < 0.0001$). (C) Morphology of the plaques formed on Vero cells by VEEV TC-83 variants from the samples harvested at 24 h p.i. from mock- and NHC-treated cells. Due to profound differences in infectious titers, different dilutions are presented.

an anti-VEEV agent. Previous studies demonstrated that NHC significantly inhibits replication of hepatitis C virus (HCV) replicon and bovine viral diarrhea virus in Huh7 and MDBK cells, respectively (22). NHC was also capable of inhibiting human norovirus replicon in HG23 cells (23), human coronavirus (24), and chikungunya virus (25). It was reasonable to expect that the antiviral effect of this nucleoside analog is not limited to these few viruses, and might also be effective against other viral species with RNA genomes, such as VEEV. We tested the effect of NHC on VEEV replication, defined optimal *in vitro* conditions for its application, and the mechanism of its antiviral activity. Our data demonstrate several important features of NHC. (i) NHC is a very potent anti-VEEV agent, with an EC_{50} below 1 μM. (ii) Most VEE virions released from the NHC-treated cells contain mutated viral genomes, which are incapable of replication. (iii) The antiviral effect of NHC is more prominent if it is applied during the first 4 h postinfection, when amplification of negative-strand RNA intermediates and G RNA takes place. (iv) The resistance to NHC develops very inefficiently and is determined by a cooperative function of multiple mutations in nsP4. Even after 20 passages of VEEV under increasing concentrations of NHC, the pool of VEEV mutants remained highly sensitive to NHC treatment.

RESULTS

NHC has a strong negative effect on infectious titers of the released VEEV TC-83. In initial experiments, we assessed the antiviral potential of NHC (Fig. 1A) by testing whether it was capable of inhibiting VEEV replication. Indeed, NHC demonstrated a strong negative effect on the replication of VEEV TC-83 in Vero cells. In the applied experimental conditions (see the legend to Fig. 1B), NHC at 1 and 2.5 μM concentrations reduced titers of released virus progeny by 2 and 4 orders of magnitude, respectively. Moreover, in the plaque assay, samples harvested from NHC-treated cells,
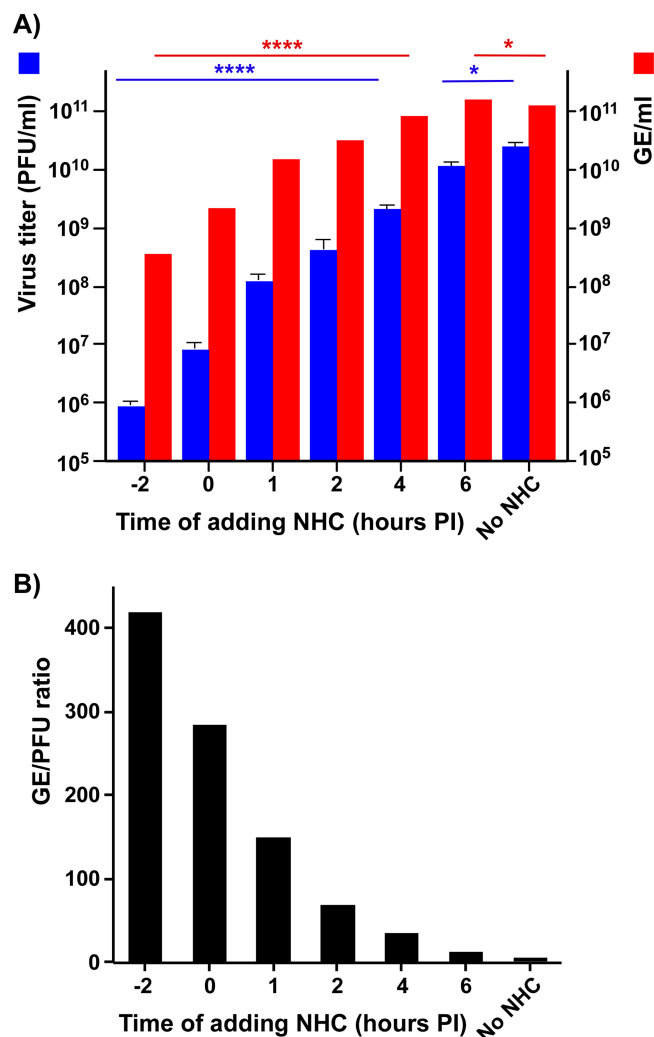
FIG 2 The antiviral effect of NHC depends on its application time. (A) Vero cells were infected with VEEV TC-83 at an MOI of 0.5 PFU/cell. At the time points indicated, cells were treated with 2 μM NHC and then harvested at 24 h p.i. Viral titers were determined using a plaque assay on Vero cells. The data are presented as mean values and standard deviations. In the same samples, the number of genome copies of VEEV TC-83 (GE/ml) was measured by qPCR. (B) GE/PFU ratio in the samples presented in panel A. This experiment was repeated twice with consistent results.

but not from the mock-treated cells, contained a large fraction of small-plaque-forming VEEV variants (Fig. 1C). The heterogeneity of plaques suggested that the antiviral effect of NHC is likely, at least partially, determined by its RNA-mutagenic activity.

Antiviral effect of NHC depends on the timing of its application. In subsequent experiments, Vero cells were infected with VEEV at a multiplicity of infection (MOI) of 0.5 PFU/cell. NHC was added to cells at 2 μM either 2 h prior to VEEV infection, at the moment of infection, or at different times postinfection (p.i.). Infectious titers of the released virus were determined at 24 h p.i. using a plaque assay (PFU/ml), and the concentrations of genome-containing viral particles in the same samples were assessed by reverse transcription-quantitative PCR (RT-qPCR) as genome equivalents (GE) per ml.

NHC was most potent when applied 2 h before infection, causing a reduction in infectious virus titers of more than 4 orders of magnitude. If it was added at later times p.i., the negative effect on released viral progeny titers gradually decreased (Fig. 2A). Addition of the compound at 6 h p.i. had a very small, <5-fold, negative effect on final infectious titers. NHC treatment prior to infection or at early times p.i. also had a negative effect on the release of genome-containing viral particles. However, the
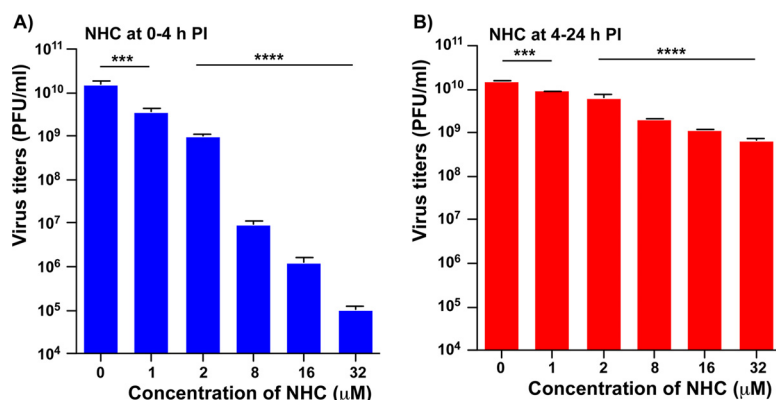
FIG 3 The first 4 h p.i. are a critical time for the antiviral effect of NHC. Vero cells in six-well Costar plates were infected at room temperature with VEEV TC-83 at an MOI of 20 PFU/cell. (A) Cells were incubated with NHC at the concentrations indicated from 0 to 4 h p.i. At 4 h p.i., the cells were washed, and media were replaced with NHC-free medium. (B) Infected cells were incubated in NHC-free medium until 4 h p.i., and then media were replaced by those supplemented with NHC at indicated concentrations. All of the samples indicated in panels A and B were harvested at 24 h p.i., and viral titers were determined by a plaque assay on Vero cells. The experiments were performed in triplicates. The reductions in viral titers in all NHC treated samples were statistically significant, as assessed by the one-way ANOVA.

measured changes in concentrations of GE in the same samples were less prominent than the decreases in the infectious titers (Fig. 2A). Accordingly, samples from the cells treated with NHC starting from 2 h prior to infection, 0 h p.i., 1 h p.i., and 2 h p.i. exhibited higher GE/PFU ratios than those obtained for mock-treated cells or in samples harvested from cells treated with NHC from 6 h p.i. (Fig. 2B). In the media from cells incubated with the compound starting from 2 h prior to infection, the GE/PFU ratio was >100-fold higher than in media harvested from mock-treated cells. This was an indication that early treatment led to release of mostly noninfectious virions. Thus, these experiments demonstrated that NHC treatment has strong negative effects on both the efficiency of genome-containing virion release and their infectivity. However, the antiviral effect of NHC is strongly dependent on the timing of its application in relation to viral infection.

To further evaluate the time-dependent effect of NHC treatment, the compound was added at different concentrations (1 to 32 μM) to the media either (i) for the first 4 h p.i. only, followed by incubation in drug-free media (Fig. 3A), or (ii) incubation in the presence of NHC started at 4 h p.i. (Fig. 3B) and continued until 24 h p.i.. All of the samples were harvested at 24 h p.i. to assess infectious titers. NHC treatment within the first 4 h caused profound reduction in infectious titers at 24 h p.i., and there was a strong dose dependence. In contrast, treatment started after 4 h p.i. caused a relatively small negative effect on the infectious titers, irrespective of NHC concentration and despite its presence in the media for a longer period of time (20 h) compared to the samples incubated with this compound for only the first 4 h p.i.

Taken together, these data strongly suggested that NHC is most effective against VEEV *in vitro* when applied early in the viral replication cycle. As a result, measuring the 50% effective concentration (EC_{50}) and other antiviral characteristics of NHC is very dependent on the time of its application and the MOI used. Therefore, for detailed evaluation of the antiviral effect of NHC on its concentration, subconfluent Vero cells were synchronously infected at an MOI of 20 PFU/cell, and drug was applied at different concentrations at 0 h p.i. The media were harvested at 24 h p.i., and the virus titers were determined by plaque assay on Vero cells. The results are presented in Fig. 4A. Based on these data, the EC_{50}, EC_{90}, and EC_{99} were 0.426, 1.036, and 2.5 μM, respectively.

In parallel experiments, we also assessed the cytotoxicity of NHC (Fig. 4B). Vero cells were incubated in the media supplemented with NHC at 0 to 200 μM for 24 h. Cell viability was assessed using Cell Titer-GLO 2.0 assay. In this range of concentrations,
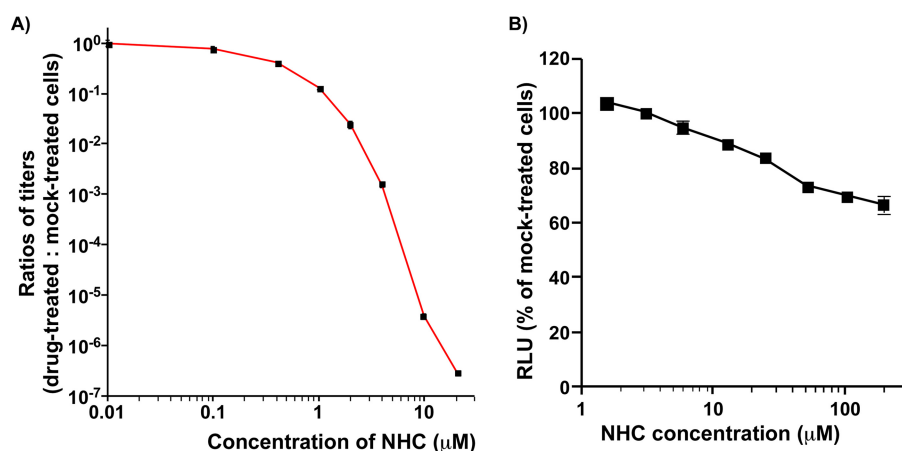
FIG 4 NHC is a potent anti-VEEV compound with low cytotoxicity. (A) Vero cells were infected with VEEV TC-83 at an MOI of 20 PFU/cell. The indicated concentrations of NHC were applied at 0 h p.i., and media were harvested at 24 h p.i. Infectious titers were determined by a plaque assay on Vero cells and normalized to those in the mock-treated samples. The experiment was performed three times. The standard deviation are too low to be visible on the plot. (B) Vero cells were incubated for 24 h with indicated concentrations of NHC in the media. Cell viability was assessed using the Cell Titer-GLO 2.0 assay. Data were normalized to those generated on the mock-treated cells. RLU, relative light units.

NHC demonstrated a cytotoxicity that was too low to determine a 50% cytotoxic concentration ($CC_{50} > 200$ μM).

NHC induces high mutation rates in VEEV G RNA. Next, we tested whether the presence of NHC increases the mutation rates of viral G RNA. Vero cells were infected with VEEV TC-83 at an MOI of 2 PFU/cell and incubated for 24 h either in NHC-free media or in media supplemented with 2 μM NHC at the time of infection. G RNAs were purified from harvested stocks, and a 941-nucleotide (nt) fragment of viral genome in both samples was amplified by RT-PCR. The PCR products were cloned into a plasmid, and for each sample, the plasmid insertions of 50 randomly selected clones were sequenced. We identified 42 mutations (8.9 mutations per 10,000 nt) in sequences derived from the virus population generated on NHC-treated cells, and only 4 mutations were detected in the sequences generated from virus harvested on mock-treated cells (0.85 mutations per 10,000 nt). Thus, within a single passage, NHC treatment at 2 μM concentration led to at least a 10-fold increase in accumulation of mutations. However, this ratio is probably even higher, since both pools likely contained equal numbers of mutations introduced by RT and PCRs. The majority of mutations acquired in the presence of NHC were transition mutations. U-to-C or C-to-U transitions were the most prevalent and were likely generated during positive-strand RNA synthesis. The number of A-to-G and G-to-A transitions was ~4-fold lower, and these likely resulted from NHC incorporation into the negative-strand RNA.

VEEV resistance to NHC develops very inefficiently. Characterization of the drug's antiviral effects requires assessing the possibility for development of resistant viral mutants. Moreover, identification of the adaptive mutations provides critical information about the mechanism of antiviral function. In this study, we passaged the cDNA-derived VEEV TC-83 20 times in the presence of incrementally increasing concentrations of NHC (see Materials and Methods for details). Drug resistance developed very inefficiently and became clearly detectable only after 15 passages, as evidenced by more efficient cytopathic effect (CPE) development in the presence of NHC. This was suggestive that the drug-resistant phenotype likely required multiple adaptive mutations, and a high resistance is probably impossible to generate. After 20 passages, we selected a viral population, which was capable of replication and CPE production in the presence of 3.2 μM NHC. Starting from passage 1, harvested virus stocks produced heterogeneous plaques, and no homogeneous viral population was found at any passage, including passage 20. This was indicative of continuous viral evolution, even after acquiring partial resistance to NHC.

After passage 20, two plaques were randomly selected from the agarose overlay supplemented with 2 μM NHC. After extraction from the agarose, plaque-purified viruses were amplified once in the presence of 1 μM NHC to avoid appearance of true or second-site revertants with an NHC-sensitive phenotype. Total RNA was isolated from Vero cells, which were used for this virus amplification. These cell-derived RNAs were used to sequence the genome fragment encoding nsP1-, nsP2-, nsP3-, and nsP4-coding genes (nt 540 to 7700 of viral G RNA). This genome fragment encodes all viral nonstructural proteins, which form a replication complex and thus are directly involved in RNA synthesis. Mutations in these genes could directly determine viral resistance to NHC.

Both plaque isolates contained large numbers of mutations. The nsP-coding sequence of plaque isolate 1 (PP1) contained 34 synonymous and nonsynonymous mutations (47.5 mutations per 10,000 nt), and the plaque isolate 2 (PP2), which was used in the following experiments, had 41 mutations in the same fragment (57.3 mutations per 10,000 nt). The mutations resulting in amino acid substitutions in the nsPs are presented in Fig. 5A. Similarly, in the PP2 genome, the RNA sequence encoding viral structural proteins contained 21 mutations (55 mutations per 10,000 nt) with 4 of them causing amino acid changes (H96R and F389L in E2; P8S and V388M in E1). These mutations in structural genes had no effect on virus infectivity, and the PP2 isolate demonstrated the same GE/PFU ratio as did the original VEEV TC-83 (see Fig. 7B). Therefore, these mutations were not further investigated. In agreement with the results described above, obtained after treating the infected cells with NHC for 24 h, all but one mutations found in viruses passaged 20 times in the presence of NHC were transition mutations, with prevalent U-to-C or C-to-U transitions (Fig. 5B). Importantly, a large number of synonymous and nonsynonymous mutations in the nsP-coding sequence were the same in both randomly selected plaque isolates. This was a strong indication that development of any resistance to NHC is likely to be a rare event and requires a cooperative/synergistic effect of more than one adaptive mutation. Such a mutant likely appeared in one of the intermediate, earlier passages; however, it continued to accumulate other mutations, which distinguished nucleotide sequences of plaque isolates selected after final passage 20.

As a control, VEEV TC-83 was passaged in parallel 20 times in the absence of NHC. After this serial passage, neither changes in the plaque sizes nor changes in virus titers were detected (data not shown). Sequencing of the nsP-coding fragment of a plaque purified after passage 20 virus identified only two mutations (2.8 mutations per 10,000 nt). Both mutations found in the virus passaged without drug were transversions. Thus, the passaging in the presence of NHC resulted in accumulation ~20-fold more mutations than in the absence of the compound. These results correlate well with the above data, showing a strong difference in the mutation rates during a single passage of VEEV TC-83 in the presence or absence of NHC.

To complete evaluation of the drug resistance development process, we tested the efficiency of reverting of the NHC-resistant isolate back to an NHC-sensitive phenotype. The PP2 isolate was passaged 20 times in Vero cells in NHC-free media. After the last passage, the resulting virus population was homogeneous in terms of plaque size, and these plaques were indistinguishable from those formed by VEEV TC-83 (see Fig. 6C). A plaque-purified variant (PREV1) from this population was used to sequence the nsP-coding genes. Surprisingly, it retained all of the PP2-specific mutations in nonstructural genes, but accumulated 12 additional mutations, from which 6 were nonsynonymous (Fig. 5A).

In the absence of NHC, PREV1 growth rates were very similar to those of the original VEEV TC-83 (Fig. 6A) and were strongly affected by the presence of NHC in the media (Fig. 6B). In side-by-side experiments, without NHC, the PP2 mutant exhibited delayed replication and achieved lower titers (Fig. 6A) compared to both wild-type (wt) VEEV and PREV1 but reproducibly yielded higher titers in NHC-containing media (Fig. 6B). Similarly, in a plaque assay when NHC was present in the agarose overlay, the PP2 mutant was capable of forming plaques in the presence of NHC at 1.2 and 2.5 μM

A)

Mutant Plaque1 (PP1)	Mutant Plaque2 (PP2)	PREV1	nsP
V263A	V263A	V263A	nsP1
V280A	V280A	V280A	
A514T	A514T	A514T	
Y15H	Y15H	Y15H	nsP2
		Q80R	
	K202E	K202E	
	V293A	V293A	
	V340M	V340M	
		D492N	
N499D	N499D	N499D	
T770A			
		I92V	nsP3
V237I			
		I359T	
T360I	T360I	T360I	
	I372T	I372T	
	S412P	S412P	
F419L			
L424S			
	S480P	S480P	
V502A	V502A	V502A	
	V119I	V119I	nsP4
	A126V	A126V	
P187S	P187S	P187S	
A189V	A189V	A189V	
I190T	I190T	I190T	
		A201V	
M347I			
C465R	C365R	C365R	
		V496A	

B)

PP1

	U	C	G	A
U		18		
C	7			
G				4
A		5		

PP2

	U	C	G	A
U		23		
C	7			
G				4
A			7	

PREV1

	U	C	G	A
U		4		
C	1			
G				3
A		4		

VEEV p20, pl. purified

	U	C	G	A
U				1
C				1
G				
A				

FIG 5 VEEV TC-83 accumulates a large number of mutations when exposed to NHC. (A) VEEV TC-83 was serially passaged in the presence of NHC (see Materials and Methods for details), and the nsP-coding fragments in the genomes of two randomly selected plaque isolates (PP1 and PP2) were sequenced. PP2 isolate was then passaged 20 times in NHC-free media, and the same nsP-coding fragment in the genome of plaque-purified variant PREV1 was sequenced. Only the nonsynonymous mutations are presented. The mutations identified in both PP1 and PP2 are highlighted in gray. Additional mutations identified in PREV1 are highlighted in red. (B) Matrixes of nucleotide substitutions identified in plaque purified variants PP1, PP2, PREV1, and plaque-purified VEEV TC-83 after 20 passages in the absence of NHC.
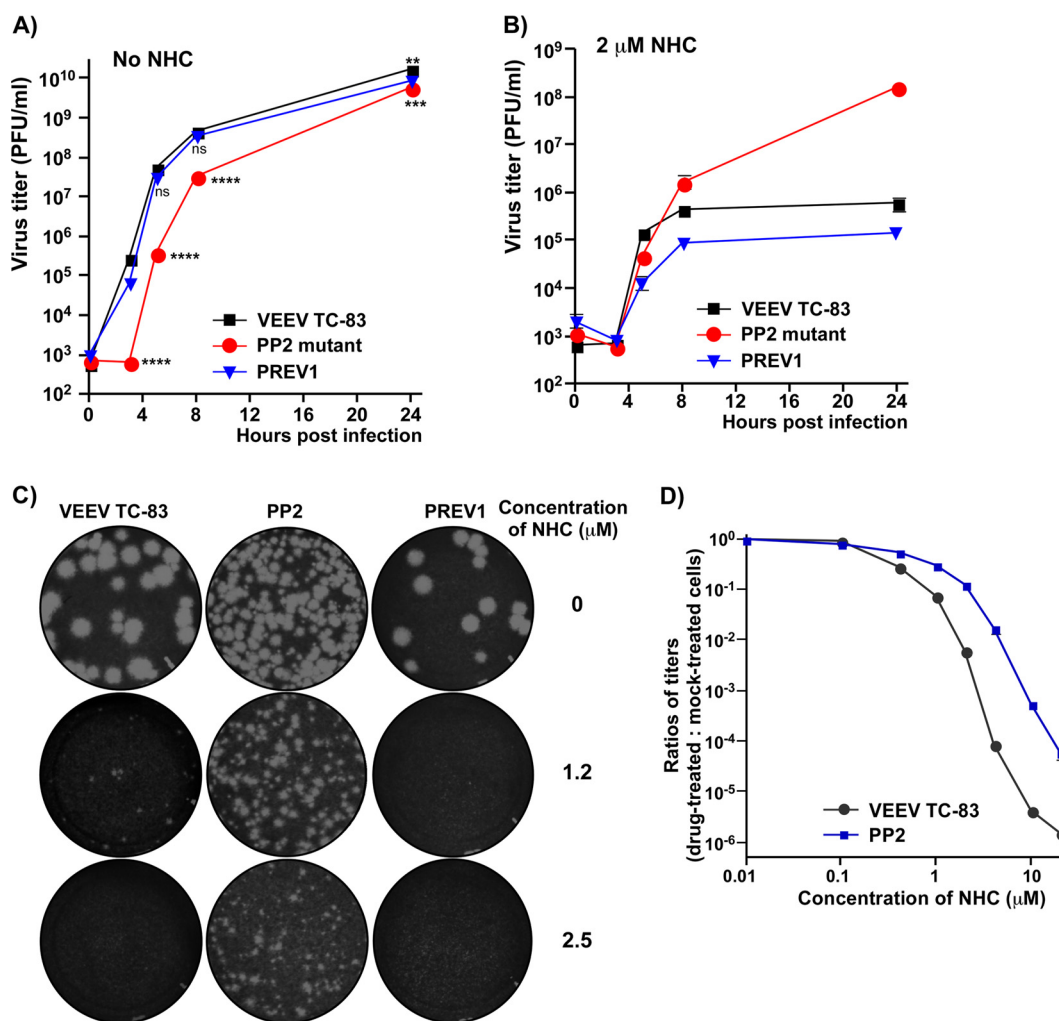
FIG 6 Drug-resistant VEEV isolate PP2 replicates more efficiently than parental VEEV TC-83 and pseudorevertant PREV1 in the presence, but not in the absence of NHC. Subconfluent Vero cells were infected with parental VEEV TC-83, selected PP2 mutant or PREV1 viruses at an MOI of 1 PFU/cell. Starting from 0 h p.i., cells were incubated either in the absence (A) or in the presence (B) of 2 μM NHC. At the indicated time points, media were harvested, and viral titers were determined using a plaque assay on Vero cells. The experiment was repeated three times. Most of the standard deviations are too small to be visible on the plots. On panel B, starting from 5 h p.i., titers of PP2 and PREV1 are significantly different from those of VEEV TC-83 and from each other ($P < 0.0001$). (C) In a standard plaque assay, cell monolayers infected with the same dilution samples were overlaid with 0.5% agarose-containing media (see Materials and Methods for details) without or with the indicated concentrations of NHC. Plaques were visualized by crystal violet staining at 2 days p.i. (D) Vero cells were infected with VEEV TC-83 and PP2 mutant at an MOI of 20 PFU/cell. The indicated concentrations of NHC were applied at 0 h p.i., and media were harvested at 24 h p.i. Infectious titers were determined by a plaque assay on Vero cells and normalized to those in the mock-treated samples. The standard deviations are too low to be visible on the plot.

concentrations. In contrast, wt VEEV TC-83 could not develop plaques in the presence of 2.5 μM NHC, and PREV1 did not produce plaques under the drug at both concentrations (Fig. 6C).

Taken together, our results demonstrated that (i) in the presence of NHC, the selected PP2 mutant replicated more efficiently than parental VEEV TC-83 and PREV1; (ii) the PP2 drug resistance was unstable and in the absence of NHC, this mutant reverted to an NHC-sensitive phenotype; (iii) the evolution to higher replication rates of the pseudorevertant PREV1 and its sensitivity to drug were the results of accumulation of additional mutations in the PP2 genome, but not the reversal of those developed under the prior NHC treatment.

NHC inhibits VEEV replication via a dual mechanism. To further evaluate the mechanism of NHC-specific inhibition of VEEV replication, we performed a detailed

comparative analysis of VEEV TC-83, the PP2 mutant, and the PREV1 pseudorevertant for their ability to produce both infectious virus and G RNA-containing viral particles. Vero cells were infected with these viruses at the same MOI and incubated either with or without 2 μM NHC added at the time of infection. At the indicated time points, media were harvested and used for assessment of both infectious titers (PFU/ml) and concentrations of released viral particles (GE/ml). The results of these experiments (Fig. 7A) demonstrate that the presence of NHC in the media caused a dramatic ($>$1,000-fold) decrease of VEEV TC-83 and PREV1 infectious titers. However, depending on the time p.i., we detected only a 5- to 50-fold decrease in PP2 infectious titers in media harvested from the drug-treated cells compared to mock-treated cells. (ii) In agreement with the results presented in Fig. 2, NHC at 2 μM had a relatively small, but readily detectable negative effect on the release of genome-containing viral particles (GE/ml) of both the original VEEV TC-83 and PREV1. For both viruses, at any time p.i., the G RNA concentrations (GE/ml) in the media of drug-treated cells were 10- to 20-fold lower than in the mock-treated controls. In contrast, the NHC-resistant PP2 mutant produced essentially the same level of particles (GE) in the presence or absence of NHC (Fig. 7A).

Thus, NHC treatment had a dual effect on parental VEEV TC-83 and PREV1 replication. This compound caused a modest decrease in virion release and a strong decrease in virion infectivity. The latter effect likely resulted from the introduction of lethal mutations into G RNA. On the other hand, in the presence of 2 μM NHC, PP2 mutant was able to release viral particles to higher infectious titers compared to VEEV TC-83 and PREV1. However, the negative effect of the compound on infectious titers of PP2, but not on particle release, was also detectable. This resulted in an increase in the PP2 GE/PFU ratio (Fig. 7B) but not to the levels detected in VEEV TC-83 and PREV1 samples. Thus, a large fraction of released PP2 virions also contained noninfectious G RNA, and this was an additional indication that the resistance of PP2 to NHC was only partial.

NHC induces rapid evolution of the VEEV population. Sequencing the plaque-purified variants provided important information about virus evolution under NHC pressure. To complement these data, we applied next-generation sequencing (NGS) to additionally characterize the effect of NHC treatment and/or virus passaging on accumulation of mutations in VEEV TC-83 pools. We sequenced genomes in virus samples harvested at passages 5, 10, 15, and 20, performed either in the absence or presence of NHC. The read sequences were aligned against the VEEV TC-83 genome and analyzed as described in Materials and Methods. The results presented in Fig. 8A, were in agreement with sequencing of the plaque-purified variants. Even after 20 passages in the absence of drug, the VEEV TC-83 population demonstrated relatively low diversity. Only 7 mutations with frequency above 5% were found after 20 passages. None of the mutations became prevalent (with frequencies above 50%). In contrast, passaging VEEV TC-83 in the presence of NHC induced high levels of mutations and led to high heterogeneity of the viral population. After passage 5, four mutations with frequencies above 5% were already present. After passage 20, more than 200 mutations with frequencies above 5% were detected in the virus pool, and 30 of them became prevalent ($>$50%). These data correlated with finding of one synonymous or nonsynonymous mutation per every 150 to 200 nt in the genomes of plaque-purified variants (Fig. 5A), which were isolated from the same passage 20 viral pool.

Using NGS, we detected the accumulation of mutations in essentially all viral genome sequences. However, it was reasonable to expect the mutations responsible for resistance to NHC to be localized in nsP4 and to become dominant by passage 20. In the NHC passage 20 stock, NGS detected four nonsynonymous nsP4-specific mutations, which were present in the viral pool with frequencies higher than 50%. Most importantly, the same mutations were identified in the plaque-purified variants, PP1 and PP2 (Fig. 5A). This was an additional indication that they may be responsible for development of resistance to NHC. Three out of four mutations, namely, P187S, A189V, and I190T, were closely located on the index finger in a three-dimensional (3D) structural model of nsP4 (see Fig. 10).
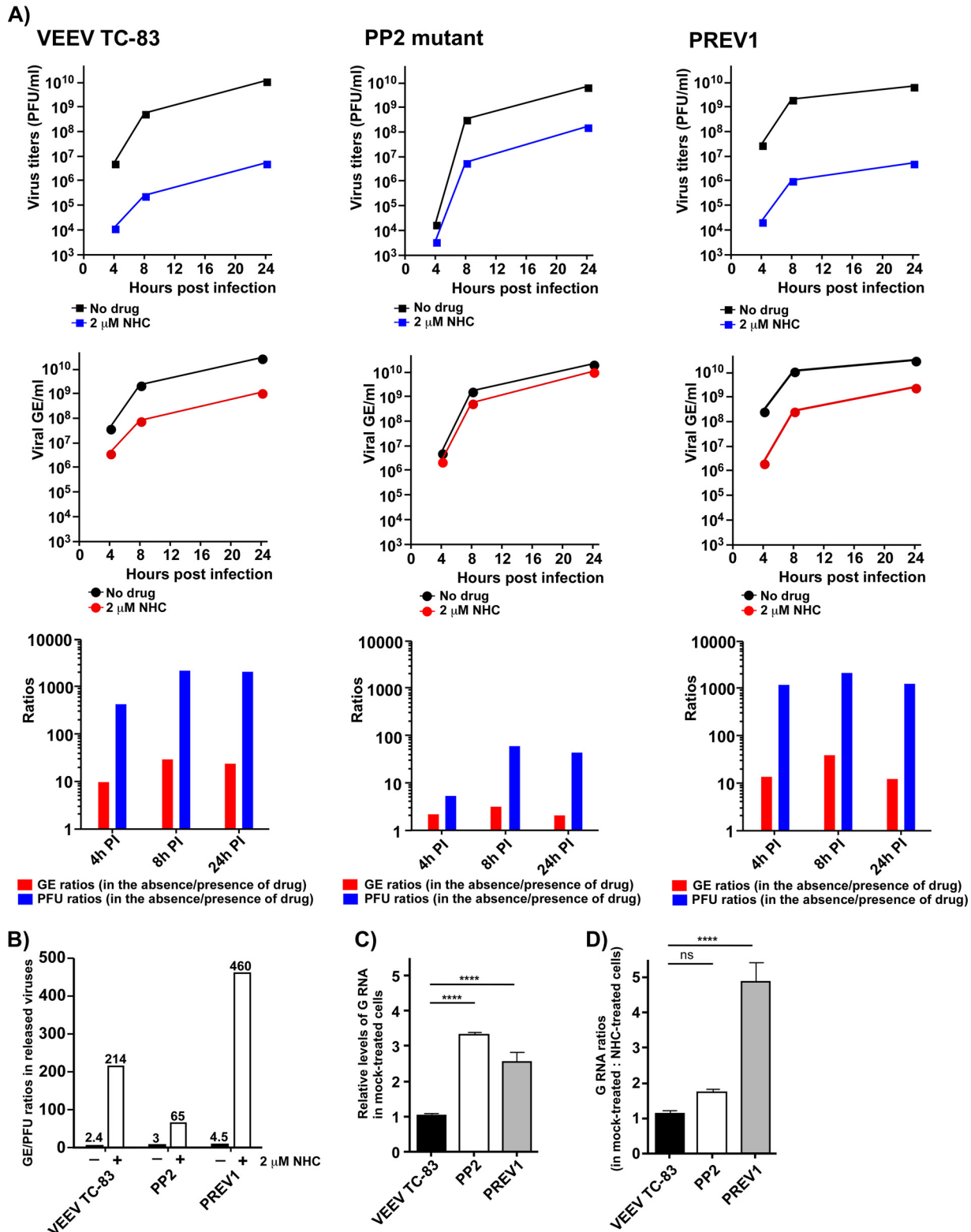
FIG 7 NHC has stronger negative effects on the release and infectivity of VEEV TC-83 and PREV1 particles than those of the PP2 mutant. A total of 5 × 10⁵ Vero cells in six-well plates were infected with VEEV TC-83, PP2, or PREV1 at an MOI of 1 PFU/cell and were incubated with or without 2 μM NHC. At the indicated time points, media were collected, and the infectious titers (PFU/ml) and concentrations of genome-containing viral particles (GE/ml) were determined by a plaque assay on Vero cells and RT-qPCR, respectively. Experiments were performed in triplicates. The standard deviations are too small to be visible on the plots. (B) GE/PFU ratios in virus samples harvested at 24 h p.i. of mock-treated and NHC-treated cells in the experiment presented in panel A. (C) Levels of viral G RNAs in the mock-treated cells at 24 h p.i. The cells were harvested after collecting the medium samples described in panel A at 24 h p.i. Data were normalized to the G RNA levels in VEEV TC-83-infected cells. (D) Ratio of G RNAs in mock-treated versus NHC-treated cells at 24 p.i. with the indicated viruses. Cells were collected in the experiment presented in panel A.
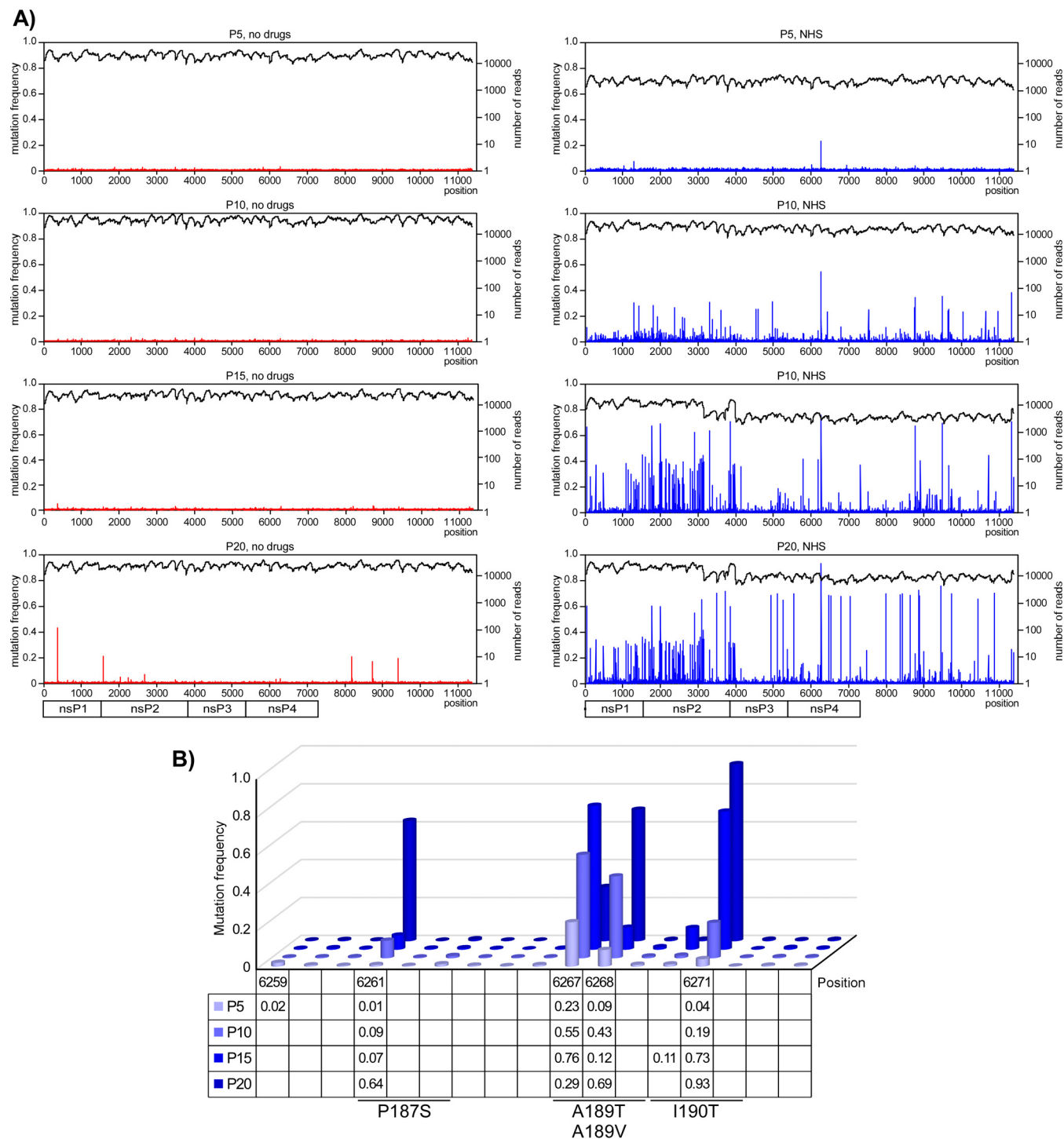
FIG 8 VEEV TC-83 passaging in the presence of increasing concentrations of NHC leads to rapid accumulation of mutations in viral pool. (A) Frequencies of mutations in viral pools at passage 5, 10, 15, and 20 in the absence or presence of NHC, determined by NGS (see Materials and Methods for details). (B) Dynamics of the increase in the frequencies of mutations at the indicated positions of VEEV nsP4.

Further analysis of the NGS data revealed an interesting dynamic in nsP4 evolution (Fig. 8B). The presence of VEEV genomes encoding a nonconservative amino acid substitution I190T steadily increased with virus passaging. After passage 20, the mutation was present in more than 90% of G RNAs. The prevalence of variants with another substitution (A189T) was 23% at passage 5 and steadily increased to 76% by passage 15. However, by passage 20, the A189T mutation was no longer prevalent and

was replaced in the virus pool by a combination of two other amino acid substitutions, P187S and A189V. The dynamics of mutation accumulation in the index finger suggested the possibility of its function in regulating nucleotide incorporation by VEEV nsP4.
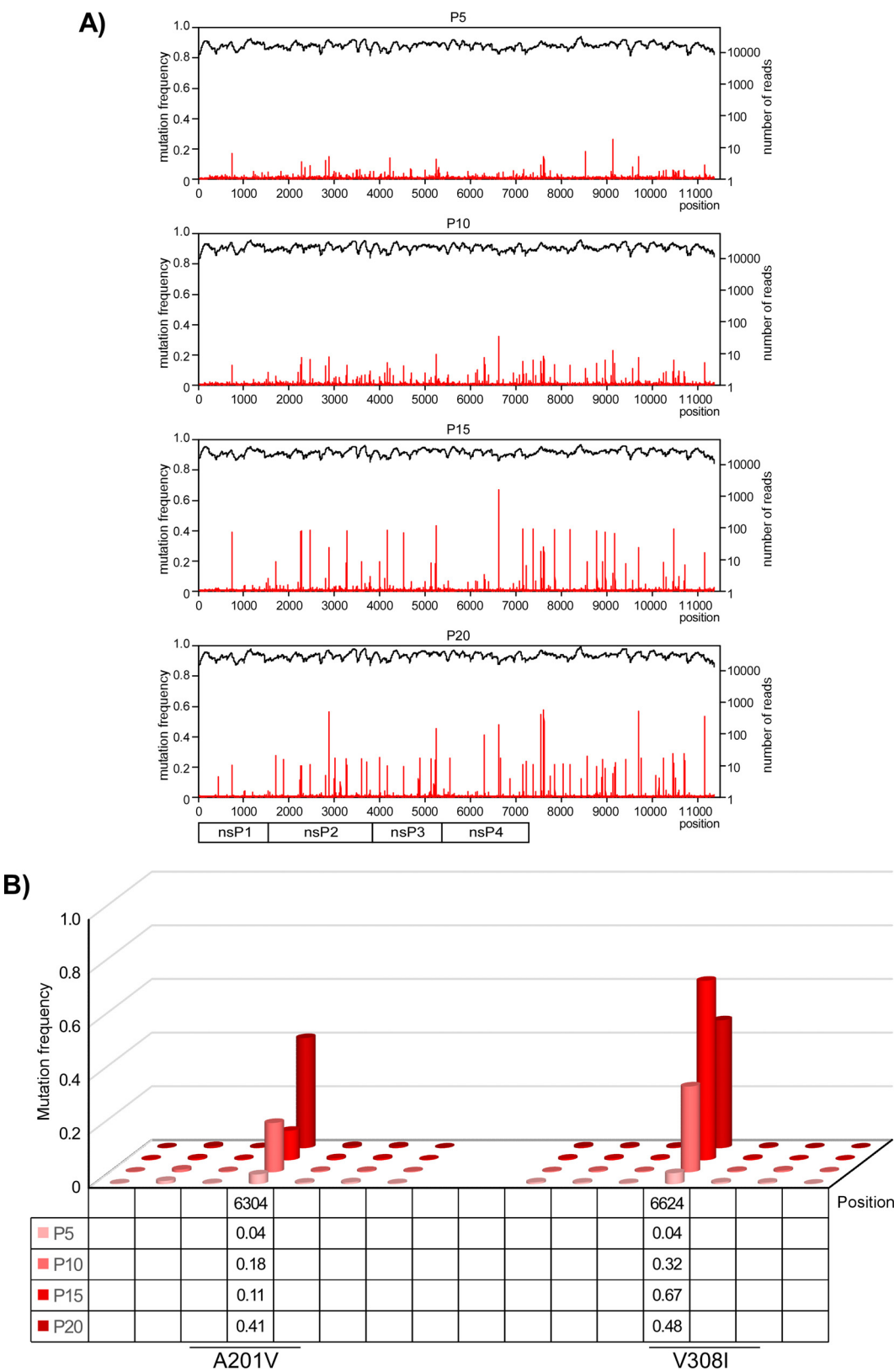
NHC-resistant VEEV variant continued to rapidly evolve in the absence of NHC. NGS was also applied for analysis of mutation accumulation in the NHC-resistant PP2 plaque isolate during its serial passage in NHC-free media. As in the above-described experiments, we sequenced population of G RNAs isolated from samples of PP2-originated viruses after passages 5, 10, 1, and 20 in drug-free media. Interestingly, in the absence of NHC, the replication complex of PP2 continued to introduce additional mutations, which were equally distributed throughout the viral genome (Fig. 9A). After passage 5, the frequencies of the detected mutations were already higher than those in similarly passaged VEEV TC-83 (Fig. 8A, left panel). Mutations continued to accumulate during the following passages, whereas the viral pools retained all of the PP2-specific mutations. These data correlated with the findings of numerous new mutations in the plaque-purified PREV1 isolate from the passage 20 stock (Fig. 5A).

At passage 20 in drug-free media, only two new prevalent mutations that led to amino acid substitutions in nsP4 (A201V and V308I) were identified (Fig. 9B). Interestingly, in the predicted 3D structure of VEEV nsP4, they were located very close to each other (Fig. 10) and to the mutations found in the NHC-resistant virus population and in the plaque isolates PP1 and PP2. Based on the frequencies of A201V and V308I mutations in the passage 20 viral pool and on the different dynamics of their appearance (Fig. 9B), it is reasonable to expect that they function independently and are present in different viral genomes. Moreover, substitution A201V, but not V308I, was identified in the PREV1 variant (Fig. 5A), which had reverted to an NHC-sensitive phenotype. Therefore, the effects of A201V on loss of resistance to NHC were analyzed further.

The identified nsP4-specific mutations are the determinants of resistance and sensitivity of selected VEEV variants to NHC. To design VEEV variants with mutated nsP4, we used the following information. The I190T mutation in VEEV nsP4 was the most prevalent in the virus pool after 20 passages in the presence of NHC (Fig. 8B). Based on the predicted 3D structure of VEEV nsP4, the second identified mutation, P187S, changed the same amino acid as that previously implicated in ribavirin resistance development by foot-and-mouth disease virus (26). Combination of I190T, P187S, and A189V mutations was identified in both the pool of NHC-resistant mutants (Fig. 8B) and the genomes of plaque-purified variants (Fig. 5). Thus, based on these data, we designed single (VEEV/P187S and VEEV/I190T) and triple (VEEV/3x) mutants (Fig. 11A) and evaluated the effects of the introduced mutations on the ability of VEEV TC-83 to replicate in the presence of NHC.

In the absence of drug, all of the reengineered mutants were viable, replicated at essentially the same rates as VEEV TC-83 (Fig. 11C), and formed large plaques in Vero cells (Fig. 11B). However, in the presence of 1.5 μM NHC in the agarose overlay (Fig. 11B), (i) the parental VEEV TC-83 formed almost undetectable, pinpoint plaques; (ii) the VEEV/P187S mutant, surprisingly, was found to be more sensitive to compound than parental VEEV TC-83 and did not form plaques at all; (iii) the VEEV/I190T mutant produced readily detectable plaques, which remained relatively small; (iv) the combination of all three mutations in nsP4 made the VEEV/3x variant capable of forming midsize plaques in the presence of NHC, which was suggestive of its higher resistance to the drug. To confirm this result, Vero cells were infected with the indicated mutants at an MOI of 2 PFU/cell, and NHC at the indicated concentrations was added to the media at the time of infection. Figure 11D presents the ratios of infectious viral titers produced in the presence or absence of NHC at 8 h p.i. As in the above-described experiments, the VEEV/I190T mutant was more resistant to NHC than the parental VEEV, VEEV/P187S was more sensitive to this compound, and the VEEV/3x mutant was the most resistant to the NHC treatment. The NGS data also suggested that during passaging in the presence of NHC (Fig. 8B), the virus population became

FIG 9 Accumulation of mutations in the genome of plaque-purified, NHC-resistant VEEV isolate PP2 (see Fig. 5) during its serial passaging in NHC-free media. (A) Frequencies of mutations in viral populations at passage 5, 10, 15, and 20, determined by NGS. (B) Dynamics of increase in mutation frequencies at the indicated positions of nsP4.
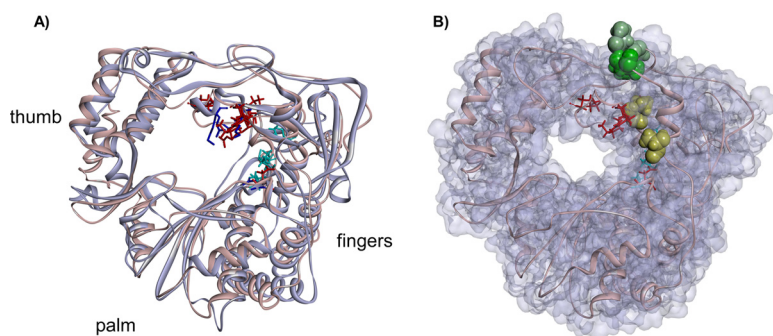
FIG 10 The mutations that lead to NHC-resistant and NHC-sensitive phenotypes of VEEV TC-83 are closely located in the 3D structure of the catalytic domain of VEEV nsP4. (A) Structural alignment of the predicted 3D structure of VEEV nsP4 RdRp domain with FMDV 3D polymerase (2E9T). The VEEV RdRp structure is presented as a solid, light red ribbon. The structure of FMDV 3D protein is presented as a solid, light blue ribbon. The amino acids involved in coordination of NTP phosphates are presented as red sticks (VEEV) or blue sticks (FMDV). The amino acids that bind RNA template are presented as turquoise sticks for both polymerases. (B) Positions of mutations identified in nsP4 of NHC-resistant and NHC-sensitive mutants of VEEV TC-83 on the predicted structure of the catalytic domain. The amino acids that were substituted in the NHC-resistant viruses are shown in medium green (I190) and light green (A189 and P187). The amino acids that were substituted in the pool of PP2 virus passaged 20 times in NHC-free media (A201V and V308I, see Fig. 9 for details) are shown in yellow.

initially enriched with the variants containing A189T mutation in nsP4. During further passaging, the latter mutation was mostly replaced in virus pool by A189V. Therefore, in additional experiments, we compared the effects of both mutations on development of virus resistance to drug. As expected, the ultimate A189V mutation induced significantly higher resistance to NHC than the early A189T mutation in nsP4 (Fig. 11E).

Analysis of the NGS data and sequencing of the PREV1 isolate suggested the possibility that the A201V mutation in nsP4 plays a critical role in reversion of PP2 to an NHC-sensitive phenotype. Indeed, cloning of A201V into the genome of the VEEV/3x mutant (Fig. 12A) had a profound negative effect on viral resistance to NHC. The VEEV/3x/A201V variant replicated in Vero cells to the same titers and at the same rates as the parental VEEV TC-83 and VEEV/3x mutant but was reproducibly less resistant to NHC than both of these viruses (Fig. 12B and C). Thus, the identified A201V mutation in nsP4 was sufficient for reverting the drug-resistant phenotype of VEEV/3x to NHC sensitive.

DISCUSSION

Currently, the most widely used nucleoside analog with the antiviral activity is ribavirin (27, 28). It demonstrates a broad-spectrum inhibitory effect against a number of RNA viruses and low cytotoxicity and functions as an RNA mutagen, since it is incorporated into virus-specific RNAs by viral RdRp (22, 28). This leads to the accumulation of random mutations in viral genomes, which either affect virus replication rates at the next round of infection or make them nonviable (29–31). One of the potential concerns about application of ribavirin is that its antiviral activity only becomes evident when this drug is applied at relatively high concentrations of 100 to 1,000 μM (32) and when it is applied hours before the beginning of infection (33). To detectably inhibit CHIKV replication *in vitro*, this drug was used at 100 μM (34) and, thus far, no antiviral effect of ribavirin has been unambiguously demonstrated for VEEV (20). Another complication of using ribavirin is that at least some viruses develop drug-resistant mutants (35). This resistance is most often determined by single point mutations in RdRp-coding sequences, and they were intensely investigated in several positive-strand RNA viruses (34, 36).

In the present study, we characterized the antiviral activity of another nucleoside analog, NHC (Fig. 1A). This compound exhibited a very strong inhibitory effect on VEEV infection in cell culture. The antiviral function was readily detectable when NHC was
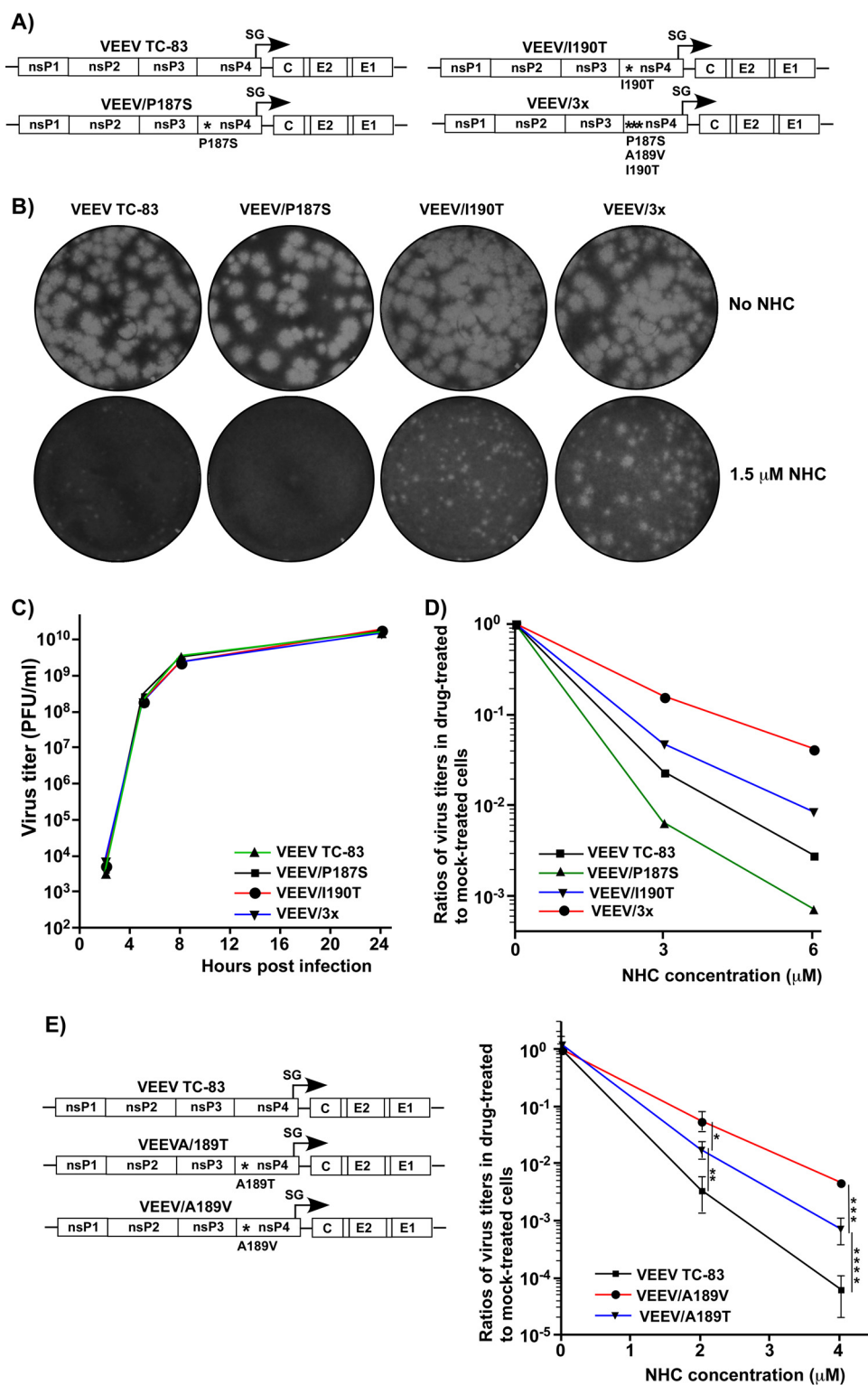
FIG 11 nsP4-specific mutations determine the resistance of VEEV replication to NHC. (A) Schematic presentations of VEEV genomes containing the indicated nsP4-specific mutations. (B) In a standard plaque assay performed on the indicated viruses, Vero cells were overlaid with 0.5% agarose-containing medium either with or without 1.5 μM NHC. After 2 days, plaques were visualized by staining with crystal violet. (C) A total of 4 $\times$ 10^5 Vero cells were infected with the indicated viruses at an MOI of 2 PFU/cell. At the indicated times p.i., media were harvested, and viral titers were determined by a plaque assay on Vero cells. (D) A total of 5 $\times$ 10^5 Vero cells were infected with the indicated viruses at an MOI of 2 PFU/cell. Cells were incubated with NHC starting from 0 h p.i. At 8 h p.i., media were harvested, and viral titers were determined by a plaque assay on Vero cells. The titers were normalized to those in the samples harvested from mock-treated cells. This experiment was repeated three times using different
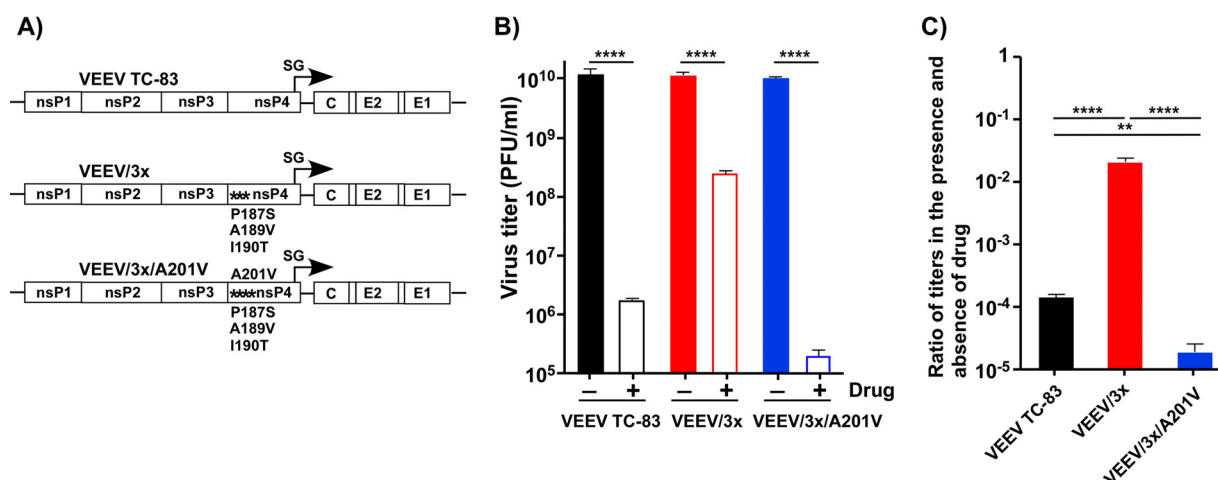
FIG 12 A201V mutation in VEEV nsP4 reverts the NHC-resistant phenotype of the VEEV/3x mutant to drug sensitive. (A) Schematic presentation of VEEV genomes containing the indicated nsP4 mutations. (B) Vero cells were infected with indicated mutant viruses at an MOI of 1 PFU/cell. Cells were incubated in the presence of 2 μM NHC starting from 0 h p.i. At 8 h p.i., media were harvested, and viral titers were determined by a plaque assay on Vero cells. (C) Titers in samples from NHC-treated cells were normalized to those in samples from mock-treated cells. This experiment was repeated three times using different concentrations of drug with consistent results. The data from one of the representative experiments are presented in this figure.

applied at 1 to 2 μM prior to, at the time of, or within 4 h after VEEV infection (Fig. 2). Previous studies showed that in cultured cells, NHC is rapidly converted into mono-, di-, and triphosphate forms, along with other metabolites, such as CTP and UTP (22, 25, 37). Because the levels of the NHC-triphosphate form (NHC-TP) were highest among the intracellular metabolites, it was proposed as the metabolite primarily responsible for the antiviral effect of NHC (22). *In vitro* experiments using purified HCV NS5B polymerase demonstrated that NHC-TP can serve as a substrate with a low efficiency of incorporation (22). Because NHC-TP can be incorporated into RNA to replace either CTP or UTP (38), one would expect the appearance of C-to-U and U-to-C transition mutations in synthesized viral G RNAs if NHC-TP is introduced into G RNA during positive-strand synthesis and A-to-G and G-to-A mutations if NHC-MP is incorporated during synthesis of the negative strand of the viral genome.

Our data support a notion that the primary antiviral effect of NHC is based on its potent RNA-mutagenic activity, which can force VEEV replication into an "error catastrophe" or "lethal defection" (39). Accordingly, viral pools released from Vero cells treated with NHC starting at early times p.i. demonstrated GE/PFU ratios that were almost 2 orders of magnitude higher than those from mock-treated cells. This was an indication that most of the released virions contained noninfectious viral genomes that were incapable of producing a spreading infection. The released viral pools also produced heterogeneous plaques, with a high proportion of these plaques being small and pinpoint in size. A >10-fold increase in the VEEV genome mutation rate was detected in the presence of 2 μM NHC compared to drug-free media. In agreement with these data, both NGS of viral pools and Sanger sequencing of the genomes in randomly selected plaque-purified variants also demonstrated that NHC treatment during VEEV replication resulted in the generation of large numbers of synonymous and nonsynonymous mutations in all of the nonstructural and structural viral genes.

On the other hand, in the presence of NHC, infected cells produced 10- to 20-fold

FIG 11 Legend (Continued)

concentrations of drug with consistent results. The data from one of the representative experiments are presented in this figure. (E) A total of 5×10^5 Vero cells were infected with the indicated viruses at an MOI of 2 PFU/cell. Cells were incubated with NHC starting from 0 h p.i. At 20 h p.i., media were harvested, and viral titers were determined by a plaque assay on Vero cells. Titers were normalized to those in the samples harvested from mock-treated cells.

fewer G RNA-containing viral particles (GE). We detected only a small decrease in G RNA accumulation in the cells treated with NHC compared to the mock-treated cells (Fig. 7D). Therefore, there is some possibility that similar to favipiravir (40), NHC can function as a direct, weak inhibitor of RdRp. However, another, more plausible explanation for less efficient release of G RNA-containing virions is that during intracellular viral replication, NHC-TP is responsible for accumulation of mutations in nonstructural and structural proteins rather than for direct inhibition of RNA synthesis. Similarly, prior *in vitro* studies using HCV RdRp did not find evidence that the presence of NHC could lead to direct inhibition of the polymerization reaction. It has also been proposed that the incorporation of NHC-TP may change the thermodynamics of RNA secondary structures and thereby affect the initiation of replication and/or protein translation (22). Although this is a considerable possibility for VEEV RdRp, such an assumption needs experimental support.

The anti-VEEV effect of NHC is dramatically more prominent when it is applied a few hours before or within the first 4 h p.i. There are two possible explanations for such temporal dependence of the inhibitory effect. First, the immature replication complex, which is composed of P123 and nsP4, is only present within the first 4 h p.i., at the amplification stage of viral RNA. In this complex, RdRp might utilize NHC-TP more efficiently than in a mature RC that contains completely processed, individual nsPs. The second and more likely possibility is that during the early stage of replication, when G RNA undergoes multiple rounds of amplification, incorporation of NHC-MP into both positive- or negative-strand RNAs generates large numbers of mutations in the viral progeny. Moreover, early in the infection, the synthesized mutated G RNAs are also translated into defective nsPs, and this in turn affects VEEV replication rates and the efficiency of particle release.

Another major characteristic of NHC is that the development of resistance to this compound by VEEV is a highly inefficient process. The difficulty in selection and the poor resistance of selected mutants suggested that (i) the acquisition of a single mutation in nsP4 has a relatively small positive effect on virus resistance to NHC and (ii) the accumulation of a few mutations appears to be required for advanced resistance to the drug. In two independent selections, one of which is presented in this study, the low-level resistance to NHC only became evident after 15 passages.

Further experiments clearly demonstrated that this low-level resistance is determined by a combination of nsP4-specific mutations. The NGS of G RNAs in viral pools at different passages, sequencing of the genomes of plaque-purified viruses and subsequent reverse genetics experiments demonstrated that resistance to NHC resulted from sequential selection of several mutations in VEEV nsP4. Acquisition of I190T substitution was likely the most critical step. It was detected as early as passage 5 (4% frequency) and became present in almost 100% of the viral genomes by passage 20 (in the presence of NHC). Moreover, the same mutation was prevalent in viral genomes after the second independent selection of NHC-resistant variants (data not shown). Although I190T substitution alone caused detectable resistance of VEEV to NHC (Fig. 11), the ultimately developed triple mutant contained a combination of P187S, A189V, and I190T substitutions in nsP4. Their presence made virus replication clearly more resistant to the drug (Fig. 11). Based on a predicted structural model of VEEV nsP4 RdRp (Fig. 10), all three mutated amino acids were located in the RdRp index finger domain near the template entrance channel. Other research teams, using a variety of picornaviruses, have previously identified several RdRp-specific mutations that generate resistance to different nucleoside analogs (32, 40–42). However, only the P44S substitution in the RdRp of foot-and-mouth disease virus (FMDV) appeared in the same position as P187S in the structural model of VEEV-specific RdRp (26). The indicated FMDV-specific mutation has been proposed to amplify the resistance of this virus to ribavirin. The authors of that study suggested that the substitution of P44S increased the frequency of ribavirin incorporation instead of guanosine by affecting the shape of the template channel and the template transition rates through the active site. This in turn resulted in a

detectable reduction of the FMDV mutant replication rates. The NHC-resistant PP2 variant selected in our study also demonstrated lower replication rates than both the original VEEV TC-83 and the drug-sensitive pseudorevertant PREV1. This suggests that less efficient RNA replication may be an important contributor to VEEV resistance to the compound. This assumption needs more detailed investigation because, in the case of PP2, the lower rate of viral replication was likely determined by a synergistic effect of numerous mutations accumulated in viral nsPs. Importantly, upon the withdrawal of NHC, the selected PP2 mutant further evolved to a more efficiently replicating phenotype. It was also acquiring mutations dramatically more efficiently than the original VEEV TC-83 in the absence of drug. At this stage, we cannot definitively distinguish whether the higher evolution rates of PP2 in the absence of NHC were the direct result of accumulation of previous mutations in nsP4 or its higher replication rates. However, the more efficiently replicating phenotype of PREV1 correlated with a complete loss of NHC resistance, and it became even more sensitive to this compound than the original VEEV TC-83.

Based on the results of NGS, after 20 passages of the NHC-resistant PP2 isolate in NHC-free media, the resulting viral pool retained all of the original PP2-specific mutations and also acquired A201V and V308I substitutions in nsP4. Based on their frequencies and the presence of only the A201V substitution in PREV1-specific nsP4, we hypothesized that A201V and V308I substitutions were likely encoded by different genomes rather than present together. Spatially, they are located close to each other and to the mutations leading to NHC resistance (Fig. 10), suggesting their possible function in both increasing the viral replication rates and lowering the resistance levels to the drug. Indeed, the addition of a single A201V-encoding mutation into the genome of NHC-resistant triple mutant (VEEV/3x) resulted in reversion to a drug-sensitive phenotype. Interestingly, in a predicted model of the nsP4 RdRp, A201 in the F motif is located next to K200, which, based on a structural alignment with FMDV 3D polymerase, may interact with the RNA template (43). Therefore, this mutation may compensate for the defect caused by a triple substitution in the index finger domain. Thus, the amino acid substitutions that lead to NHC resistance and its reversion possibly affect the interaction of template RNA with VEEV-specific RdRp.

In summary, this study demonstrated several key features of NHC. (i) NHC is a very potent anti-VEEV compound. (ii) NHC induces high mutation rates in the genome of replicating VEEV. (iii) NHC application has negative effects on both the release of viral particles and their infectivity. (iv) The antiviral effect of NHC is most prominent when it is applied at early times postinfection, during the rapid amplification of negative and positive-strand RNAs and assembly of replication complexes. (v) VEEV resistance to NHC develops very inefficiently. Even a low-level resistance requires acquisition of more than one mutation in VEEV nsP4. (vi) The development of such mutations correlates with lower replication rates of the virus. (vii) In the absence of NHC, the resistant mutants of VEEV revert to an NHC-sensitive phenotype and higher replication rates by acquiring additional mutations in nsP4. Taken together, our data suggest that NHC is a very promising and potent anti-VEEV agent that can likely also be used against other alphavirus infections.

MATERIALS AND METHODS

NHC was synthesized at Emory Institute for Drug Development. Its synthesis and additional characterization will be presented elsewhere.

Cell cultures. Vero cells were obtained from the American Type Culture Collection (Manassas, VA). BHK-21 cells were kindly provided by Paul Olivo (Washington University, St. Louis, MO). These cell lines were maintained at 37°C in alpha minimum essential medium supplemented with 10% fetal bovine serum and vitamins.

Plasmid constructs. The original plasmids containing the infectious cDNAs of VEEV TC-83 were described elsewhere (44). Mutations were introduced into nsP4 using standard PCR-based techniques. Schematic representations of all of the modified genomes are presented in the corresponding figures. The sequences of the plasmids and details regarding the cloning procedures can be provided upon request.

***In vitro* RNA transcription and transfection.** Plasmids with the VEEV TC-83 genome and its derivatives were purified by ultracentrifugation in CsCl gradients. They were then linearized using a MluI restriction site located downstream of the poly(A) sequence. RNAs were synthesized by SP6 RNA polymerase in the presence of a cap analog, as described elsewhere (45). Electroporation of BHK-21 cells by *in vitro*-synthesized RNA was performed under previously described conditions (45, 46). In all of the experiments, viral titers were determined by a plaque assay on Vero cells as described elsewhere (47).

Selection of VEEV TC-83 mutants. A total of 2.5×10^6 Vero cells in 100-mm dishes were infected at an MOI of 1 PFU/cell with either original, electroporation-derived VEEV TC-83 or stocks harvested at the prior passage. The starting concentration of NHC was 1 μM, and it was gradually increased by passage 20 to 3.2 μM. Viral stocks were harvested at each passage after developing signs of a CPE, either at 24 or 48 h p.i. After the final passage, the plaques were randomly selected from the agarose cover, supplemented with 2 μM NHC. Viruses from two agarose plugs (PP1 and PP2) were extracted and used to infect Vero cells in the presence of 1 μM NHC to avoid the possible selection of true and pseudo-evertants. At 24 h p.i., cells were harvested for RNA isolation and sequencing of viral genomes, and media were used as stocks for further analysis of viral isolates. One of the plaque-purified variants, PP2, was additionally passaged 20 times in Vero cells in the absence of NHC. During this serial passage, the volume of inoculum harvested from the previous passage was being gradually decreased from 100 to 0.01 μl. After the last passage, the viral population was homogeneous in terms of plaque size. One of the plaques (PREV1) was selected, and the extracted virus was used to infect Vero cells. Harvested medium was used for further experiments, and RNA from the infected cells was used for sequencing of viral nsP genes. Passaging of the original VEEV TC-83 in the absence of NHC was performed in parallel under the same conditions. After passage 20, one of plaques was also isolated, and the nsP-coding sequence was sequenced. For all isolates, DNA fragments were synthesized using RT-PCR and sequenced in the UAB Heflin Center Genomics Core Facility.

RT-qPCR. The viral RNA was isolated using ZR viral RNA kit (Zymo Research) from 100-μl portions of medium samples harvested at different time points p.i. with the indicated viruses grown in the absence or presence of NHC. As an internal control for normalization of the data, 10 μl of media containing the same amount of Sindbis virus (SINV) was added to each sample before RNA purification. VEEV- and SINV-specific cDNAs were synthesized using a QuantiTect reverse transcription kit (Qiagen) and further used for quantitative PCR (qPCR) analysis using VEEV and SINV nsP2-specific primers. The qPCRs were performed in triplicates using SsoFast EvaGreen Supermix (Bio-Rad) and a CFX96 real-time PCR detection system (Bio-Rad). The specificities of the products were tested by measuring their melting temperatures, and the data were normalized to the mean threshold cycle of the SINV control in each sample. Averages from three reactions and standard deviations were calculated and plotted on the graphs. Total cellular RNAs were isolated from infected Vero cells using a ZR viral RNA kit. cDNAs synthesis and qPCR analyses were performed using the above-described protocols, and the data were normalized to the concentrations of 18S rRNA present in the same samples.

NGS. Viral G RNAs were isolated from 0.6-ml portions of viral stocks indicated in the corresponding figures using ZR viral RNA or Direct-Zol RNA Mini Prep kits (Zymo Research). Purified viral RNAs were used to prepare NGS libraries using an Agilent SureSelect strand-specific mRNA library kit according to the manufacturer's instructions (Agilent, Santa Clara, CA), except that poly(A) selection was omitted. Briefly, 40-ng portions of viral RNAs were randomly fragmented with cations and heat, followed by the first-strand cDNA synthesis using random primers with the inclusion of actinomycin D (2.4 ng/μl final concentration). Second-strand cDNA was synthesized using standard techniques for stranded libraries. Adaptors were ligated for indexing to allow for multiplexing during sequencing. The size selection and purification of the libraries was performed using the Agilent 2100 bioanalyzer. The average amplicon length was 400 bp. Prior to cluster generation, the cDNA libraries were quantitated using qPCR in a Roche LightCycler 480 with a Kapa Biosystems kit for Illumina library quantitation (Kapa Biosystems, Woburn, MA). The 300-bp paired-end sequencing was performed on a MiSeq Illumina machine in the UAB Heflin Center Genomics Core Facility.

Illumina BaseSpace was used for base-calling and read demultiplexing. Trim Galore (v0.4.1) was used to remove adaptor contaminants and reads shorter than 15 bp and to trim low-quality bases (Q-score < 30). The high-quality, trimmed, paired-end fastq reads were then merged into one single-end read fastq file. The single-end trimmed fastq reads were then aligned using BWA-MEM (v0.7.15-r1140) to the VEEV reference genome in order to create the aligned SAM file. Naive Variant Caller (Galaxy, v0.0.2) was used to generate a variant file from the sorted BAM file on all positions of the VEEV genome. To create the count lists containing the number of bases seen at each position, Variant Annotator (Galaxy, v1.2) was used on the Naive Variant Caller's vcf file. The list was further processed in Excel to account for all possible mutations at each position and to generate figures. Table 1 presents the total and aligned read numbers.

Analysis of viral replication. A total of 5×10^5 Vero cells were seeded into six-well Costar plates and infected at MOIs indicated in the figure legends. NHC was added to the cells at the indicated times, media were harvested, and viral titers in the samples were determined by a plaque assay on Vero cells as described elsewhere (47).

Statistical analysis. Statistical analysis was performed using GraphPad Prism 7 software. The two-way analysis of variance (ANOVA) with the Tukey correction was used for statistical analysis of virus replication rates. The one-way ANOVA with the Dunnett's correction was used for statistical analysis of infectious virus titers and concentrations of GE. The data are presented as means $\pm$ the standard

TABLE 1 Number of total and mapped reads

Sample	Virus	Treatment	Passage	Total no. of raw reads	No. (%) mapped reads to the genome
W0	VEEV TC-83	None	0	1,694,499	1,473,387 (86.95)
W5	VEEV TC-83	None	5	1,932,410	1,320,488 (68.33)
W10	VEEV TC-83	None	10	3,055,210	2,575,881 (84.31)
W15	VEEV TC-83	None	15	2,436,142	1,720,526 (70.63)
W20	VEEV TC-83	None	20	2,239,203	1,697,248 (75.80)
d5	VEEV TC-83	NHC	5	1,583,429	168,026 (10.61)
d10	VEEV TC-83	NHC	10	2,748,574	1,291,652 (46.99)
d15	VEEV TC-83	NHC	15	1,312,641	456,518 (34.78)
d20	VEEV TC-83	NHC	20	2,102,043	949,366 (45.16)
r5	VEEV TC-83, PP2	None	5	1,588,152	1,171,668 (73.78)
r10	VEEV TC-83, PP2	None	10	1,893,413	1,699,941 (89.78)
r15	VEEV TC-83, PP2	None	15	2,059,806	1,691,743 (82.13)
r20	VEEV TC-83, PP2	None	20	2,438,228	2,170,0771 (89.03)

deviations. The differences with $P > 0.05$ were considered nonsignificant (ns). P values of <0.05, <0.01, 0.001, and 0.0001 are indicated by asterisks (*, **, ***, and ****, respectively).

REFERENCES

1. Strauss JH, Strauss EG. 1994. The alphaviruses: gene expression, replication, evolution. Microbiol Rev 58:491–562.
2. Zacks MA, Paessler S. 2010. Encephalitic alphaviruses. Vet Microbiol 140:281–286. https://doi.org/10.1016/j.vetmic.2009.08.023.
3. Weaver SC, Ferro C, Barrera R, Boshell J, Navarro JC. 2004. Venezuelan equine encephalitis. Annu Rev Entomol 49:141–174. https://doi.org/10.1146/annurev.ento.49.061802.123422.
4. Gibbs EP. 1976. Equine viral encephalitis. Equine Vet J 8:66–71. https://doi.org/10.1111/j.2042-3306.1976.tb03293.x.
5. Gibney KB, Robinson S, Mutebi JP, Hoenig DE, Bernier BJ, Webber L, Lubelczyk C, Nett RJ, Fischer M. 2011. Eastern equine encephalitis: an emerging arboviral disease threat, Maine, 2009. Vector Borne Zoonotic Dis 11:637–639. https://doi.org/10.1089/vbz.2010.0189.
6. Go YY, Balasuriya UB, Lee CK. 2014. Zoonotic encephalitides caused by arboviruses: transmission and epidemiology of alphaviruses and flaviviruses. Clin Exp Vaccine Res 3:58–77. https://doi.org/10.7774/cevr.2014.3.1.58.
7. Weaver SC. 2001. Venezuelan equine encephalitis, p 539–548. In Service MW (ed), The encyclopedia of arthropod-transmitted infections. CAB International, Wallingford, UK.
8. Weaver SC. 2001. Eastern equine encephalitis, p 151–159. In Service MW (ed), The encyclopedia of arthropod-transmitted infections. CAB International, Wallingford, UK.
9. Reisen WK. 2001. Western equine encephalitis, p 558–563. In Service MW (ed), The encyclopedia of arthropod-transmitted infections. CAB International, Wallingford, UK.
10. Reed DS, Larsen T, Sullivan LJ, Lind CM, Lackemeyer MG, Pratt WD, Parker MD. 2005. Aerosol exposure to western equine encephalitis virus causes fever and encephalitis in cynomolgus macaques. J Infect Dis 192:1173–1182. https://doi.org/10.1086/444397.
11. Lemm JA, Rice CM. 1993. Roles of nonstructural polyproteins and cleavage products in regulating Sindbis virus RNA replication and transcription. J Virol 67:1916–1926.
12. Shirako Y, Strauss JH. 1994. Regulation of Sindbis virus RNA replication: uncleaved P123 and nsP4 function in minus strand RNA synthesis whereas cleaved products from P123 are required for efficient plus strand RNA synthesis. J Virol 185:1874–1885.
13. Gorchakov R, Frolova E, Sawicki S, Atasheva S, Sawicki D, Frolov I. 2008.

A new role for ns polyprotein cleavage in Sindbis virus replication. J Virol 82:6218–6231. https://doi.org/10.1128/JVI.02624-07.
14. Chung DH, Jonsson CB, Tower NA, Chu YK, Sahin E, Golden JE, Noah JW, Schroeder CE, Sotsky JB, Sosa MI, Cramer DE, McKellip SN, Rasmussen L, White EL, Schmaljohn CS, Julander JG, Smith JM, Filone CM, Connor JH, Sakurai Y, Davey RA. 2014. Discovery of a novel compound with anti-Venezuelan equine encephalitis virus activity that targets the nonstructural protein 2. PLoS Pathog 10:e1004213. https://doi.org/10.1371/journal.ppat.1004213.
15. Schroeder CE, Yao T, Sotsky J, Smith RA, Roy S, Chu YK, Guo H, Tower NA, Noah JW, McKellip S, Sosa M, Rasmussen L, Smith LH, White EL, Aube J, Jonsson CB, Chung D, Golden JE. 2014. Development of (E)-2-((1,4-dimethylpiperazin-2-ylidene)amino)-5-nitro-N-phenylbenzamide, ML336: novel 2-amidinophenylbenzamides as potent inhibitors of Venezuelan equine encephalitis virus. J Med Chem 57:8608–8621. https://doi.org/10.1021/jm501203v.
16. Selvam P, Vijayalakshimi P, Smee DF, Gowen BB, Julander JG, Day CW, Barnard DL. 2007. Novel 3-sulphonamido-quinazolin-4(3H)-one derivatives: microwave-assisted synthesis and evaluation of antiviral activities against respiratory and biodefense viruses. Antivir Chem Chemother 18:301–305. https://doi.org/10.1177/095632020701800506.
17. Kehn-Hall K, Narayanan A, Lundberg L, Sampey G, Pinkham C, Guendel I, Van Duyne R, Senina S, Schultz KL, Stavale E, Aman MJ, Bailey C, Kashanchi F. 2012. Modulation of GSK-3β activity in Venezuelan equine encephalitis virus infection. PLoS One 7:e34761. https://doi.org/10.1371/journal.pone.0034761.
18. Madsen C, Hooper I, Lundberg L, Shafagati N, Johnson A, Senina S, de la Fuente C, Hoover LI, Fredricksen BL, Dinman J, Jacobs JL, Kehn-Hall K. 2014. Small molecule inhibitors of Ago2 decrease Venezuelan equine encephalitis virus replication. Antiviral Res 112:26–37. https://doi.org/10.1016/j.antiviral.2014.10.002.
19. Julander JG, Bowen RA, Rao JR, Day C, Shafer K, Smee DF, Morrey JD, Chu CK. 2008. Treatment of Venezuelan equine encephalitis virus infection with (−)-carbodine. Antiviral Res 80:309–315. https://doi.org/10.1016/j.antiviral.2008.07.002.
20. Markland W, McQuaid TJ, Jain J, Kwong AD. 2000. Broad-spectrum antiviral activity of the IMP dehydrogenase inhibitor VX-497: a comparison with ribavirin and demonstration of antiviral additivity with alpha

interferon. Antimicrob Agents Chemother 44:859–866. https://doi.org/10.1128/AAC.44.4.859-866.2000.

21. Lundberg L, Pinkham C, de la Fuente C, Brahms A, Shafagati N, Wagstaff KM, Jans DA, Tamir S, Kehn-Hall K. 2016. Selective inhibitor of nuclear export (SINE) compounds alter New World alphavirus capsid localization and reduce viral replication in mammalian cells. PLoS Negl Trop Dis 10:e0005122. https://doi.org/10.1371/journal.pntd.0005122.

22. Stuyver LJ, Whitaker T, McBrayer TR, Hernandez-Santiago BI, Lostia S, Tharnish PM, Ramesh M, Chu CK, Jordan R, Shi J, Rachakonda S, Watanabe KA, Otto MJ, Schinazi RF. 2003. Ribonucleoside analogue that blocks replication of bovine viral diarrhea and hepatitis C viruses in culture. Antimicrob Agents Chemother 47:244–254. https://doi.org/10.1128/AAC.47.1.244-254.2003.

23. Costantini VP, Whitaker T, Barclay L, Lee D, McBrayer TR, Schinazi RF, Vinje J. 2012. Antiviral activity of nucleoside analogues against norovirus. Antivir Ther 17:981–991. https://doi.org/10.3851/IMP2229.

24. Pyrc K, Bosch BJ, Berkhout B, Jebbink MF, Dijkman R, Rottier P, van der Hoek L. 2006. Inhibition of human coronavirus NL63 infection at early stages of the replication cycle. Antimicrob Agents Chemother 50:2000–2008. https://doi.org/10.1128/AAC.01598-05.

25. Ehteshami M, Tao S, Zandi K, Hsiao HM, Jiang Y, Hammond E, Amblard F, Russell OO, Merits A, Schinazi RF. 2017. Characterization of β-D-N^4-hydroxycytidine as a novel inhibitor of chikungunya virus. Antimicrob Agents Chemother 61:e02395-16. https://doi.org/10.1128/AAC.02395-16.

26. Agudo R, Ferrer-Orta C, Arias A, de la Higuera I, Perales C, Perez-Luque R, Verdaguer N, Domingo E. 2010. A multi-step process of viral adaptation to a mutagenic nucleoside analogue by modulation of transition types leads to extinction-escape. PLoS Pathog 6:e1001072. https://doi.org/10.1371/journal.ppat.1001072.

27. Beaucourt S, Vignuzzi M. 2014. Ribavirin: a drug active against many viruses with multiple effects on virus replication and propagation: molecular basis of ribavirin resistance. Curr Opin Virol 8:10–15. https://doi.org/10.1016/j.coviro.2014.04.011.

28. Freistadt MS, Meades GD, Cameron CE. 2004. Lethal mutagens: broad-spectrum antivirals with limited potential for development of resistance? Drug Resist Updat 7:19–24. https://doi.org/10.1016/j.drup.2003.12.003.

29. Crotty S, Maag D, Arnold JJ, Zhong W, Lau JY, Hong Z, Andino R, Cameron CE. 2000. The broad-spectrum antiviral ribonucleoside ribavirin is an RNA virus mutagen. Nat Med 6:1375–1379. https://doi.org/10.1038/82191.

30. Crotty S, Cameron C, Andino R. 2002. Ribavirin's antiviral mechanism of action: lethal mutagenesis? J Mol Med 80:86–95. https://doi.org/10.1007/s00109-001-0308-0.

31. Crotty S, Gohara D, Gilligan DK, Karelsky S, Cameron CE, Andino R. 2003. Manganese-dependent polioviruses caused by mutations within the viral polymerase. J Virol 77:5378–5388. https://doi.org/10.1128/JVI.77.9.5378-5388.2003.

32. Pfeiffer JK, Kirkegaard K. 2003. A single mutation in poliovirus RNA-dependent RNA polymerase confers resistance to mutagenic nucleotide analogs via increased fidelity. Proc Natl Acad Sci U S A 100:7289–7294. https://doi.org/10.1073/pnas.1232294100.

33. Crotty S, Cameron CE, Andino R. 2001. RNA virus error catastrophe: direct molecular test by using ribavirin. Proc Natl Acad Sci U S A 98:6895–6900. https://doi.org/10.1073/pnas.111085598.

34. Coffey LL, Beeharry Y, Borderia AV, Blanc H, Vignuzzi M. 2011. Arbovirus high fidelity variant loses fitness in mosquitoes and mice. Proc Natl Acad Sci U S A 108:16038–16043. https://doi.org/10.1073/pnas.1111650108.

35. Vignuzzi M, Stone JK, Andino R. 2005. Ribavirin and lethal mutagenesis of poliovirus: molecular mechanisms, resistance, and biological implications. Virus Res 107:173–181. https://doi.org/10.1016/j.virusres.2004.11.007.

36. Ferrer-Orta C, Sierra M, Agudo R, de la Higuera I, Arias A, Perez-Luque R, Escarmis C, Domingo E, Verdaguer N. 2010. Structure of foot-and-mouth disease virus mutant polymerases with reduced sensitivity to ribavirin. J Virol 84:6188–6199. https://doi.org/10.1128/JVI.02420-09.

37. Hernandez-Santiago BI, Beltran T, Stuyver L, Chu CK, Schinazi RF. 2004. Metabolism of the anti-hepatitis C virus nucleoside β-D-$N4$-hydroxycytidine in different liver cells. Antimicrob Agents Chemother 48:4636–4642. https://doi.org/10.1128/AAC.48.12.4636-4642.2004.

38. Les A, Adamowicz L, Rode W. 1993. Structure and conformation of N^4-hydroxycytosine and N^4-hydroxy-5-fluorocytosine: a theoretical ab initio study. Biochim Biophys Acta 1173:39–48. https://doi.org/10.1016/0167-4781(93)90240-E.

39. Tejero H, Montero F, Nuno JC. 2016. Theories of lethal mutagenesis: from error catastrophe to lethal defection. Curr Top Microbiol Immunol 392:161–179. https://doi.org/10.1007/82_2015_463.

40. Delang L, Segura Guerrero N, Tas A, Querat G, Pastorino B, Froeyen M, Dallmeier K, Jochmans D, Herdewijn P, Bello F, Snijder EJ, de Lamballerie X, Martina B, Neyts J, van Hemert MJ, Leyssen P. 2014. Mutations in the chikungunya virus nonstructural proteins cause resistance to favipiravir (T-705), a broad-spectrum antiviral. J Antimicrob Chemother 69:2770–2784. https://doi.org/10.1093/jac/dku209.

41. Kempf BJ, Peersen OB, Barton DJ. 2016. Poliovirus polymerase Leu420 facilitates RNA recombination and ribavirin resistance. J Virol 90:8410–8421. https://doi.org/10.1128/JVI.00078-16.

42. Sierra M, Airaksinen A, Gonzalez-Lopez C, Agudo R, Arias A, Domingo E. 2007. Foot-and-mouth disease virus mutant with decreased sensitivity to ribavirin: implications for error catastrophe. J Virol 81:2012–2024. https://doi.org/10.1128/JVI.01606-06.

43. Ferrer-Orta C, Arias A, Perez-Luque R, Escarmis C, Domingo E, Verdaguer N. 2007. Sequential structures provide insights into the fidelity of RNA replication. Proc Natl Acad Sci U S A 104:9463–9468. https://doi.org/10.1073/pnas.0700518104.

44. Michel G, Petrakova O, Atasheva S, Frolov I. 2007. Adaptation of Venezuelan equine encephalitis virus lacking 51-nt conserved sequence element to replication in mammalian and mosquito cells. Virology 362:475–487. https://doi.org/10.1016/j.virol.2007.01.009.

45. Gorchakov R, Hardy R, Rice CM, Frolov I. 2004. Selection of functional 5′ cis-acting elements promoting efficient Sindbis virus genome replication. J Virol 78:61–75. https://doi.org/10.1128/JVI.78.1.61-75.2004.

46. Liljeström P, Lusa S, Huylebroeck D, Garoff H. 1991. In vitro mutagenesis of a full-length cDNA clone of Semliki Forest virus: the small 6,000-molecular-weight membrane protein modulates virus release. J Virol 65:4107–4113.

47. Volkova E, Frolova E, Darwin JR, Forrester NL, Weaver SC, Frolov I. 2008. IRES-dependent replication of Venezuelan equine encephalitis virus makes it highly attenuated and incapable of replicating in mosquito cells. Virology 377:160–169. https://doi.org/10.1016/j.virol.2008.04.020.